M&C 2017 - International Conference on Mathematics & Computational Methods Applied to Nuclear Science & Engineering, Jeju, Korea, April 16-20, 2017, on USB (2017)

Effect of pressure gradient in the connection region on the stability of edge pedestal

S. K. Kim[1], Y. S. Na[1] and O. J. Kwon[2]

[1]*Department of Nuclear Engineering, Seoul National University, Seoul 151-744, Korea*
[2]*Department of Physics, Daegu University, Gyeongsan 38453, Gyeongbuk, Korea*

Abstract - *We have numerically investigate the dependence of pedestal properties such as the pedestal height and the pedestal width on the pressure gradient (α_i) in the connection region. We use MISHKA, an ideal MHD stability code and EPED1, a predictive model of the edge pedestal to analyze the edge stability and predict its structure. As a result, improvement of pedestal properties and stability can be achieved by reducing α_i. Also, the pedestal width and height can be increased by shafranov shift. From this result, we suggest the strategy to improve the edge pedestal. It is possible to increase the pedestal height and width by increasing the core pressure and adjusting the peaking of the core pressure profile.*

I. INTRODUCTION

The width of the plasma edge pedestal, formed by the transport barrier, and the pressure at the top of pedestal (pedestal height) strongly affect the performance of fusion plasmas. To achieve the plasma of desired performance, effective prediction and optimization of the edge pedestal are required.

However, the improvement of the pedestal pressure and width still has many difficulties and understanding of its physics remains as a challenge because various plasma conditions are related to the characteristics of the pedestal structure [1]. In previous studies [2, 3], the pressure gradient at the centre of pedestal was mainly considered as a major factor that determines the pedestal stability. However, the edge instability is non-local [1, 4] and therefore, α_i (pressure gradient at the connection region between the core and the pedestal) also can play an important role on the pedestal stability and its performance.

For this purpose, we have investigated the effect of α_i at so-called “no man’s land” on the pedestal properties (connection region). We have used the EPED1 model [5], an edge predictive model which is based on the peeling-ballooning mode (PBM) [6, 7] and the kinetic ballooning mode (KBM) [3, 6], to predict and understand the behaviour of the edge pedestal in terms of pressure gradient in the connection region. A fixed boundary code, HELENA [8] is used in constructing the plasma equilibrium.

In this paper, we firstly discussed the role of edge stability on pedestal structure. The effect of pressure gradient in the connection region on the edge stability was also investigated in following section. After then, we examined the behaviour of edge pedestal structure according to pressure gradient at the connection region. Finally, we suggested the strategies to improve the edge pedestal with core profile control based on our results in last section.

II. STABILITY ANALYSIS

1. Effect of edge stability on the pedestal structure

In general H-mode plasmas, the pedestal height and the width rise together as the edge transport barrier forms which

$$\Delta_{ped} = 0.072\beta_{p,ped}^2 \qquad (1)$$

is generally understood to be related with the suppression of the long wavelength drift turbulence via the sheared $E \times B$ flow. However, the KBM turbulence can occur when the pressure gradient at the edge pedestal exceeds onset conditions. Since KBM onset condition is only weakly dependent on the $E \times B$ shear, the constraint it imposes on edge gradients can be approximately described as Eq.(1) without considering turbulence suppression in the pedestal region.
Here, $\beta_{p,ped}$ is poloidal beta at the pedestal top and Δ_{ped} is the width of edge pedestal in normalized poloidal flux coordinate (ψ_N). The KBM turbulence causes very strong transport, and thus $\beta_{p,ped}$ is limited by Δ_{ped}.

As the edge pedestal builds up, the pressure and current increases until PBM becomes unstable. PBM is a rapidly growing ideal MHD instability which causes the collapse of the pedestal leading to edge localized modes. Therefore, it determines the point where the further pedestal growth is prohibited. width of the edge pedestal. As a non-local mode, its onset can be found with a numerical MHD stability code.

Fig 1 shows the schematic description of how KBM and PBM constraints determine the pedestal height and width. In the beginning, the pedestal height and width grow along the KBM constraint (blue line) with edge turbulence suppression. When the pedestal continues to grow (following blue line), the PBM condition (orange line) is reached, and the pedestal structure is determined when the PBM constraint and the KBM constraint meet (orange star). Furthermore, we can say that more stable PBM means large pedestal height and width. For example, as edge stability improves with changes in various plasma parameters and profiles, the PBM onset line moves up in the Fig 1 (orange to green line), and the pedestal can grows further, resulting in improved height and width (orange to green star).

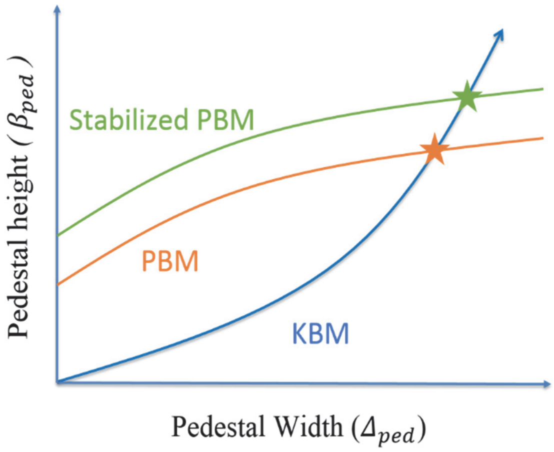

Fig 1. PBM (orange and green line) and KBM (blue line) constraints on the $\Delta_{ped} - \beta_{ped}$ space. The edge pedestal initially grows from the bottom to the upper region by following the KBM line and stops when it reaches the PBM constraint. Therefore, the intersection point between the KBM and the PBM line corresponds to the maximum pedestal height and width.

2. Effect of pressure gradient in the connection region on the PBM stability

The pressure gradient in the edge pedestal region is one of the destabilizing sources of PBM, and its growth rate increases with the magnitude of the pressure gradient. In order to investigate the effect of the pressure gradient in the connection region between core and pedestal on the PBM stability, we constructed several plasma equilibria in which the pedestal structure and the pressure at magnetic axis (P_0) are the same while the profile between them is varied. Tangent hyperbolic form of the edge pedestal [4] and the Sauter's model for bootstrap current [10] are employed to calculate the numerical plasma equilibria. The plasma parameters and shape used in the calculation are shown in Table I.

Examples of pressure profiles and pressure gradient profiles we have used in the calculations are shown in Fig 2. The pressure gradient at the connection region decreases as the pressure peaking increases when the P_0 is fixed. The stability of the edge pedestal was analyzed with MISHKA, the ideal MHD stability code [11].

The pedestal stability analysis was conducted for toroidal mode (n) = 3-20 which is the typical range of PBM. We found that the growth rate and mode structure of PBM changes with α_i. We defined α_i as Eq. (2) to represent the pressure gradient in the connection region corresponding to the normalized pressure gradient (α) at $\psi_N = 1 - 2\Delta_{ped}$ [12].

$$\alpha = -\frac{2\mu_0 \partial V/\partial\psi}{(2\pi)^2}\left(\frac{V}{2\pi^2 R_c}\right)^{\frac{1}{2}} \frac{\partial P}{\partial\psi}\bigg|_{\psi_N=1-2\Delta_{ped}} \qquad (2)$$

In Eq. (2), V is the plasma volume, R_c is the geometric center of the poloidal flux contour, P is the plasma pressure, and ψ is the poloidal flux. Smaller α_i flatter pressure profile in the connection region.

The PBM becomes more destabilized as α_i increases as shown in Fig 3. The growth rate decreased faster as α_i decreased. Especially, the change in the higher mode n was relatively larger than that in the lower n cases. For example, the growth rate of n = 5 decreased by 30% as α_i decreased from 0.12 to 0.06 while that of n = 15 was reduced by 80%. Since the pressure gradient has a greater effect on the ballooning component than the peeling one, the high n-

Table I. Plasma parameters of the model equilibrium

Variables	Values	Units
Major radius	3	[m]
Inver aspect ratio	0.3	
Triangularity	0.4	
Elongation	1.8	
Toroidal field	2.8	[T]
Plasma current	1.4	[MA]
Core pressure	4.2×10^4	[Pa]
Pedestal top pressure	4.9×10^3	[Pa]
Pedestal width	0.04	
Pedestal top density	2.8×10^{19}	$[m^{-3}]$
Effective charge number	1.5	

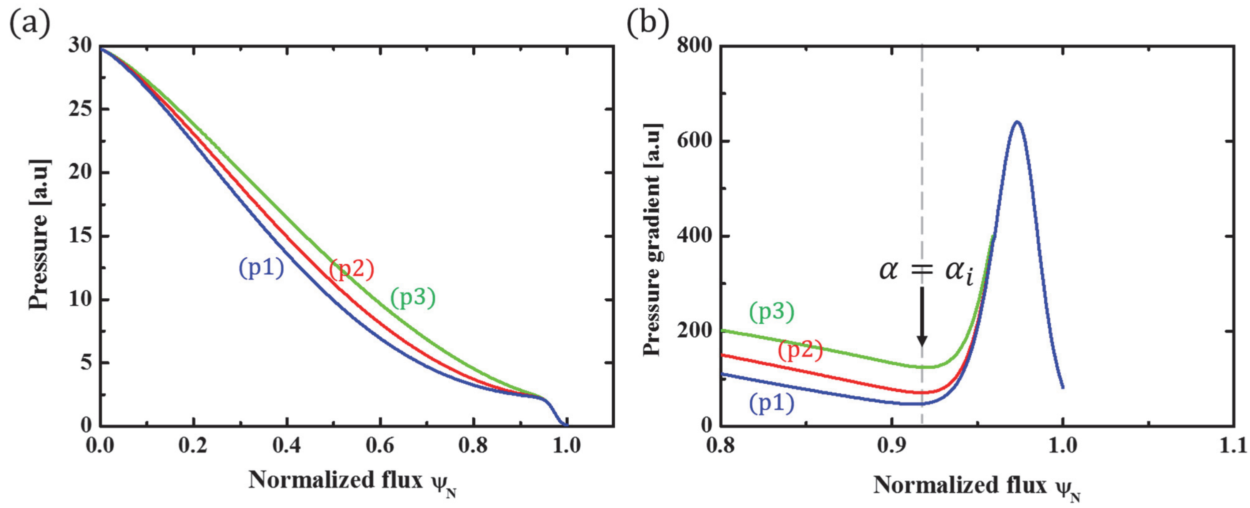

Fig 2. Three pressure profiles, p1-3, (a) and corresponding gradients (b) with the same pedestal structure and P_0 but different pressure gradient in the connection region

mode, which is dominated by the ballooning component, appears to be more sensitive to α_i. The mode structure of PBM (n = 5) is also shown in Fig 4. The structure of PBM becomes narrower as α_i increases from 0.06 to 0.12 in Fig 4. It is also consistent with previous study [13, 14]. This tendency proves the interaction between the pressure gradient in the connection region and the PBM. Even if the pressure profile in the pedestal remains the same, the stability of the edge PBM is affected by α_i. As α_i decreases, the destabilizing source in the connection region is reduced while that in the edge remains the same. This makes the growth rate and the mode width of the PBM decrease.

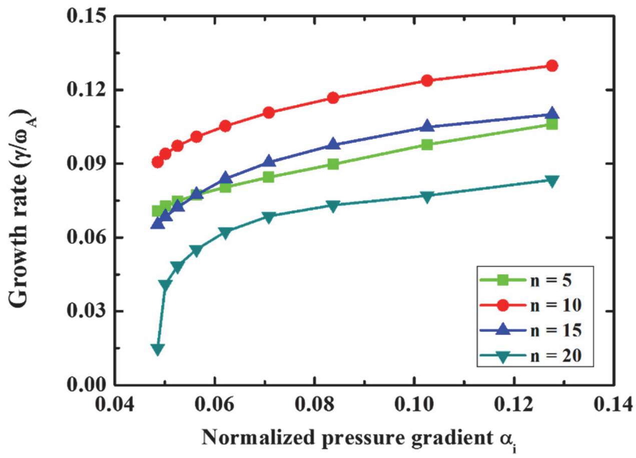

Fig 3. Growth rate of PBM with different α_i. It shows that PBM with the higher mode n is more sensitive to α_i.

III. RESULTS

1. Effect of α_i on the pedestal structure

To investigate the effect of α_i on the pedestal structure, we used EPED1 [3] to predict the pedestal height and the width for various α_i. EPED1 was applied to the target plasma shown in Table I, and the change of the pedestal was calculated by varying α_i and P_0. The reason for changing P_0 in this work is to distinguish the effect of shafranov shift (Δ_{sh}) and α_i on the pedestal, where Δ_{sh} can be expressed as Eq. (3) in simple geometry [15].

$$\Delta_{sh} \propto \beta_p + \frac{l_i}{2} \tag{3}$$

When P_0 is fixed, poloidal beta increases with α_i and consequently Δ_{sh} is reduced. Previous studies have shown that as the Δ_{sh} increases, the stability and structure of the pedestal improves significantly [16, 17]. Therefore, α_i and Δ_{sh} should be separately considered in our study to clearly see the role of α_i in edge pedestal. The width and the height of the pedestal determined by the EPED1 for different α_i and Δ_{sh} are shown in Fig 5.

As shown in the Fig 5, the height and the width of the pedestal increase as decreasing α_i. When Δ_{sh} is fixed, the height and the width of the pedestal rise by 10% and 25%, respectively, as α_i decreased from 0.12 to 0.06. This tendency is consistent with previous experiment results [18, 19]. In addition, the pedestal is greatly improved as Δ_{sh}

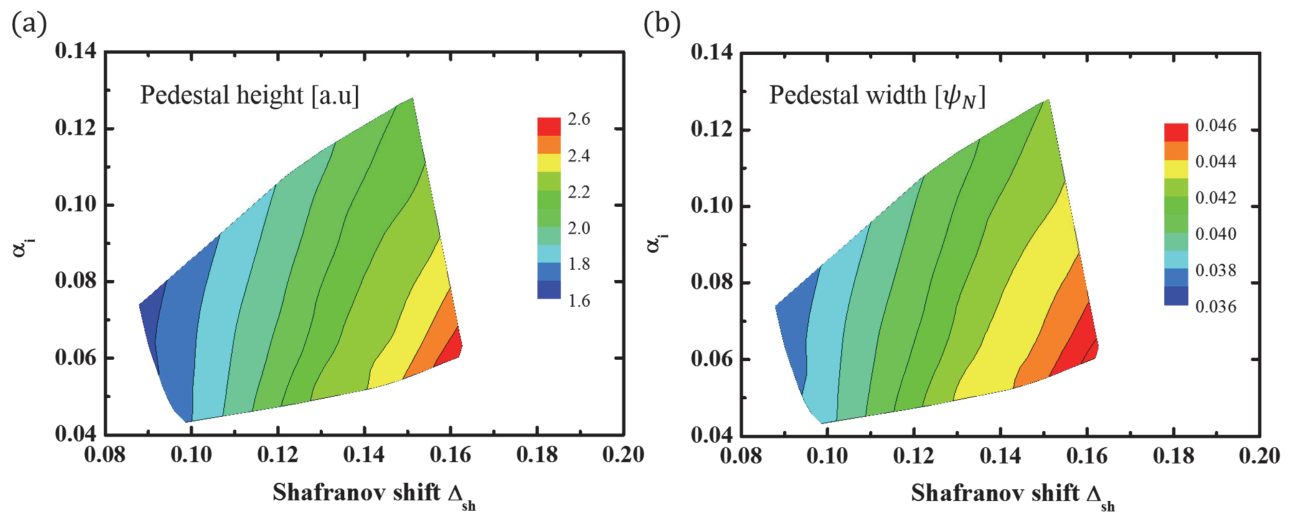

Fig 5. Pedestal height (a) and width (b) for different Δ_{sh} and α_i. Pedestal height and width both increases with Δ_{sh} and decreases as α_i increases.

increases. For example, the pedestal height increases by 30% as $\Delta_{\rm sh}$ changes from 0.1 to0.14 while α_i is fixed at 0.08. This behavior of the edge pedestal with Δ_{sh} is also consistent to previous studies [20, 21] and experiment results [22-25]. These tendencies of the pedestal structure on α_i and Δ_{sh} can be understood with their stabilization effect on PBM (see Fig 1).

2. Strategies to optimize the pedestal structure

According to the previous analysis, pedestal height and width can be improved by adjusting α_i and Δ_{sh}. Since $\Delta_{\rm sh}$ is proportional to global poloidal beta (β_p) and internal inductance (l_i), we can control Δ_{sh} and α_i through changing the core pressure profile. The relationship between the core profile and the pedestal is simplified in Fig 6 for better understanding. In this figure, ∇P_i is the pressure gradient at $\psi_N = 1 - 2\Delta_{ped}$. In addition, blue line and red line mean the positive and the negative effect, respectively.

As shown in Fig 6, β_p and l_i increase with P_0 (while ∇P_i is fixed), resulting in larger Δ_{sh}. In the case of ∇P_i, β_p increases with ∇P_i while l_i decreases because the current density profile peaking is reduced by ∇P_i. α_i also increases with ∇P_i by its definition. As a result, we can say that large P_0 is favorable to the edge pedestal as it increases Δ_{sh} so to stabilize the pedestal stability. However, effects of ∇P_i on the pedestal structure is not simple. Since ∇P_i can simultaneously increase α_i and Δ_{sh} that have opposite effects on the edge pedestal, pedestal height and width will not change monotonically with respect to ∇P_i. Therefore, it would exist optimal ∇P_i that can maximize the pedestal height and width.

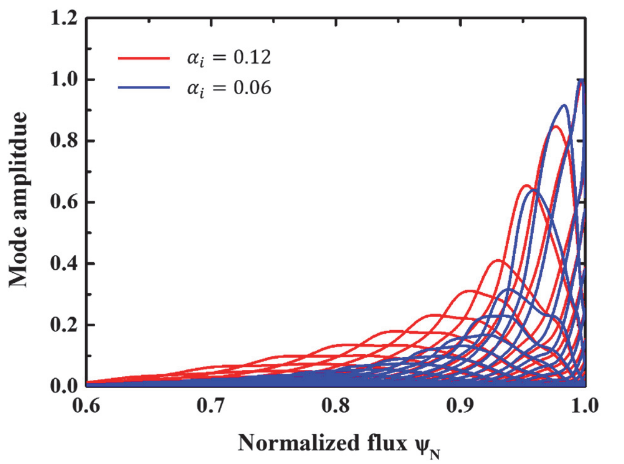

Fig 4. Mode structure of PBM for n = 5. Red line and blue line correspond to $\alpha_i = 0.12$ and 0.06, respectively. It is shown that PBM in smaller α_i has a narrower mode structure.

IV. CONCLUSIONS

We have analyzed the effect of the pressure gradient in the connection region on the edge stability. The stability of the pedestal is improved as $\alpha_{\rm i}$ decreases. It turns out that PBM is stabilized with $\alpha_{\rm i}$ through the mode interaction

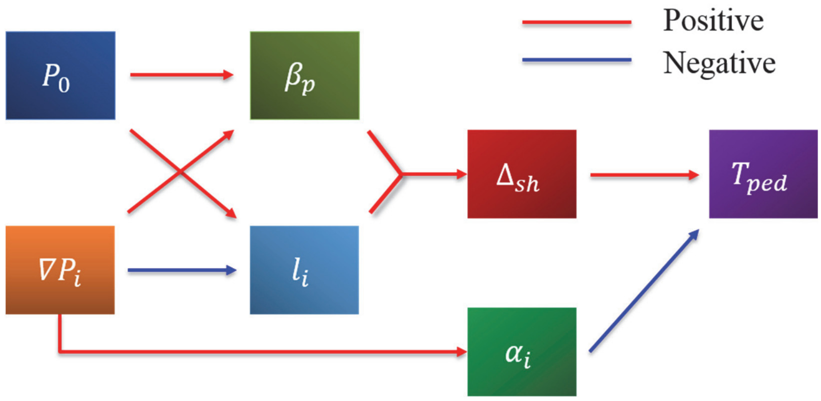

Fig 6. Schematic diagram of correlation between the core profile (P_0 and ∇P_i) and the pedestal height and width. Blue line corresponds to positive effect while red line means opposite.

between the mode in the edge pedestal and the connection region. Furthermore, we tested the effect of α_i in the pedestal structure, and found that the height and width of the pedestal can be improved by reducing α_i. We also found the consistency between our results and experimental findings [18, 19].

By considering each role of α_i and Δ_{sh} in the pedestal stability, we suggest the strategy to find the core pressure profile that can optimize the pedestal structure. From our analysis, it is found that the pedestal structure can be improved by increasing P_0 and adjusting ∇P_i. In other words, we can improve the pedestal performance through adjusting the profile peaking. We expect this approach can be used in designing future high performance tokamak plasmas owing to the improved edge pedestal. Further work to understand effect of α_i on various plasma is planned.

ACKNOWDLEGMENT

The first author would like to express the deepest gratitude to the Fusion and Plasma Application Laboratory (FUSMA) Team at Seoul National University for their kind support and fruitful discussions for this paper.

REFERENCES

1. J. W. Connor, *Plasma Phys. Control. Fusion,* 40, 191 (1998).
2. T. Onjun et al., *Physics of Plasmas*, 9, 5018 (2002).
3. A. Diallo et al., *Nucl. Fusion,* 53, 093026 (2014).
4. P. B. Snyder et al., *Phys. Plasma,* 9, 2037 (2002).
5. P. B. Snyder et al., *Phys. Plasma,* 16, 056118 (2009).
6. J. W. Connor et al., *Phys. Plasma*, 5, 2687 (1998).
7. P. B. Snyder et al., *Plasma Phys. Control. Fusion,* 46, A131 (2004).
8. F. Jenko et al., *Plasma Phys. Control. Fusion*, 43, A141 (2001).
9. G. T. A Huysmans et al., *"HELENA Installation and User Guide"* 96-228, Euratom (1996).
10. O. Satuter et al., *Physics of Plasmas,* 6, 2834 (1999).
11. A.B. Mihailovskii et al., *Plasma Phys. Rep.*, 23, 844 (1997).
12. R.L. Miller et al., *Plasma Phys. Control. Fusion*, 40, 753 (1998).
13. N. Hayashi et al., *Nucl. Fusion*, 51, 073015 (2001).
14. N. Aiba et al., *Journal of Physics: Conference Series*, 123, 012008 (2008).
15. L.L.Lao, et al., *Phys.Fluids*, 24, 1431 (1981).
16. P.B. Snyder et al., *Nucl. Fusion*, 47, 961 (2007).
17. P.B. Snyder et al., *Nucl. Fusion*, 49, 085035 (2009).
18. N. Oyama et al., *Nucl. Fusion*, 50, 64014 (2010).
19. Y. Kamada et al., *Plasma Phys. Control. Fusion,* 44, 279 (2002).
20. J.W. Connor et al., *Plasma Phys. Control. Fusion*, 58, 085002 (2016).
21. C.F. Maggi et al., *Nucl. Fusion*, 47, 535 (2007).
22. A.W. Leonard, *Journal of Physics:Conference Series,* 123, 012001 (2008).
23. H. Urano et al., *Nucl. Fusion*, 48, 045008 (2008).
24. C.F. Maggi et al., *Nucl. Fusion*, 50, 025023 (2010).
25. I.T. Champman et al., *Nucl. Fusion*, 55, 013004 (2015).